ORIGINAL ARTICLE

Journal of Cachexia, Sarcopenia and Muscle 2019; **10**: 1102–1115
Published online 29 May 2019 in Wiley Online Library (wileyonlinelibrary.com) **DOI:** 10.1002/jcsm.12448

Small-molecule-mediated chemical knock-down of MuRF1/MuRF2 and attenuation of diaphragm dysfunction in chronic heart failure

Volker Adams[1]*, T. Scott Bowen[2], Sarah Werner[3], Peggy Barthel[1], Christina Amberger[3], Anne Konzer[4,5], Johannes Graumann[4,5], Peter Sehr[6], Joe Lewis[6], Jan Provaznik[6], Vladimir Benes[6], Petra Büttner[3], Alexander Gasch[7], Norman Mangner[1], Christian C. Witt[7], Dittmar Labeit[7,8], Axel Linke[1] & Siegfried Labeit[7,8]

[1]*Laboratory of Molecular and Experimental Cardiology, TU Dresden, Heart Center Dresden, Dresden, Germany,* [2]*School of Biomedical Sciences, University of Leeds, Leeds, UK,* [3]*University Clinic of Cardiology, Heart Center Leipzig, Leipzig, Germany,* [4]*Scientific Service Group Biomolecular Mass Spectrometry, Max Planck Institute for Heart and Lung Research, Bad Nauheim, Germany,* [5]*German Centre for Cardiovascular Research (DZHK), Partner Site Rhine-Main, Rhine-Main, Germany,* [6]*European Molecular Biology Laboratory, Heidelberg, Germany,* [7]*Medical Faculty Mannheim, University of Heidelberg, Heidelberg, Germany,* [8]*Myomedix GmbH, Neckargemünd, Germany*

Abstract

Background Chronic heart failure (CHF) leads to diaphragm myopathy that significantly impairs quality of life and worsens prognosis. In this study, we aimed to assess the efficacy of a recently discovered small-molecule inhibitor of MuRF1 in treating CHF-induced diaphragm myopathy and loss of contractile function.

Methods Myocardial infarction was induced in mice by ligation of the left anterior descending coronary artery. Sham-operated animals (sham) served as controls. One week post-left anterior descending coronary artery ligation animals were randomized into two groups—one group was fed control rodent chow, whereas the other group was fed a diet containing 0.1% of the compound ID#704946—a recently described MuRF1-interfering small molecule. Echocardiography confirmed development of CHF after 10 weeks. Functional and molecular analysis of the diaphragm was subsequently performed.

Results Chronic heart failure induced diaphragm fibre atrophy and contractile dysfunction by ~20%, as well as decreased activity of enzymes involved in mitochondrial energy production ($P < 0.05$). Treatment with compound ID#704946 in CHF mice had beneficial effects on the diaphragm: contractile function was protected, while mitochondrial enzyme activity and up-regulation of the MuRF1 and MuRF2 was attenuated after infarct.

Conclusions Our murine CHF model presented with diaphragm fibre atrophy, impaired contractile function, and reduced mitochondrial enzyme activities. Compound ID#704946 rescued from this partially, possibly by targeting MuRF1/MuRF2. However, at this stage of our study, we refrain to claim specific mechanism(s) and targets of compound ID#704946, because the nature of changes after 12 weeks of feeding is likely to be complex and is not necessarily caused by direct mechanistic effects.

Keywords Muscle wasting; Diaphragm; Chronic heart failure; Cardiac cachexia; Mitochondrial metabolism; MuRF1

Received: 29 November 2018; Revised: 15 April 2019; Accepted: 17 April 2019
**Correspondence to: Volker Adams, Laboratory for Molecular and Experimental Cardiology, TU Dresden, Heart Center Dresden, Fetscherstrasse 74, 01307 Dresden, Germany. Email: volker.adams@mailbox.tu-dresden.de*

Introduction

Skeletal muscle wasting and weakness develops in several clinical conditions including chronic heart failure (CHF), pulmonary hypertension, cancer, immobilization, and sepsis. In CHF, this loss of muscle mass and function occurs in both limb and respiratory muscle and is associated with exercise intolerance, dyspnoea, and prognosis.[1–4] Therefore, reducing muscle wasting as a therapeutic intervention has the potential to modulate quality of life and reduce mortality.

Mechanistically, the activation of so-called atrogins leading to enhanced muscle protein degradation, via the ubiquitin proteasome system (UPS) or autophagosome, is a central step[5–7] in muscle wasting. In this process, the activation of the muscle ring finger protein 1 (MuRF1) is believed to drive the poly-ubiquitylation of proteins scheduled for degradation via the UPS.[8,9] The central role of MuRF1 in modulating muscle mass is further supported by observations of up-regulated MuRF1 expression in numerous clinical conditions associated with muscle wasting,[5,10] as well as after pharmacological intervention (e.g. induction of muscle atrophy by glucocorticoids, inflammatory cytokines, or reactive oxygen species),[11–13] while its inactivation can partially abolish fibre atrophy.[11,12,14] Accordingly, significant effort has been invested to down-regulate MuRF1 therapeutically, for example, by a small-molecule inhibition,[15] adenoviral-mediated knock-down,[16,17] or by exercise training,[18] where down-regulation in expression correlated with reduced muscle wasting.

We recently described a small molecule (compound ID#704946, molecular weight 490 Da) that inhibited MuRF1 expression/activity *in vivo* and was able to attenuate skeletal muscle atrophy and dysfunction in mice treated with monocrotaline to induce right ventricular hypertrophy and subsequent cardiac cachexia.[19] In that earlier study, the compound ID#704946 was given 1 week before monocrotaline treatment was initiated, complicating the interpretation of therapeutic applicability. In the present study, we therefore addressed the question of compound ID#704946's efficacy in a more clinically relevant cardiac disease model [myocardial infarction (MI)-induced heart failure] and a setting of secondary prevention (first treatment dose post-MI). Because of the key role MuRF1 plays in muscle atrophy following cardiac failure, we hypothesized that compound feeding may influence muscle wasting and loss of function in this clinically relevant animal model. Our results indicate muscle atrophy and dysfunction as partially reversed in compound-treated animals and the phenotypic rescue to be mechanistically associated with a protection of mitochondrial function as documented by metabolic energetics and proteomic homeostasis.

Materials and methods

Animals and study design

C57/BL6 female mice (n = 70) underwent an MI to induce CHF or sham surgery, where a surgical silk suture ligated the left anterior descending coronary artery (LAD) as previously described.[20,21] One week after LAD ligation, echocardiography was performed to confirm MI, and only mice with a large infarct [left ventricular ejection fraction (LVEF) $<$20%] were subsequently randomized into either receiving normal chow (CHF, n = 11) or chow supplemented with compound (0.1% of compound ID#704946, CHF + 704946, n = 12) as recently described.[19] Sham animals that underwent surgery but where the LAD was not ligated served as controls and were fed normal chow (sham, n = 15). Nine weeks after randomization, echocardiography was repeated, and animals were sacrificed to collect tissues for functional and molecular characterization (*Figure* 1A). All experiments and procedures were approved by the local Animal Research Council, University of Leipzig, and the Landesbehörde Sachsen (TVV 36/15).

Echocardiography and histology of the heart

As previously described,[20] echocardiography was performed in M-mode at 1 and 10 weeks post-surgery, with left ventricular end-diastolic (LVEDD) and systolic (LVESD) diameters assessed to allow calculation of left ventricular (LV) fractional shortening (LVFS = [LVEDD − LVESDLVEDD] × 100). At sacrifice, the medial portion of the heart was fixed in 4% phosphate-buffered saline (PBS)–buffered formalin, and sections (2 μm) stained with Picosirius red were then mounted on glass slides for subsequent analysis. A computer imaging software (Analysis 3.0, Olympus Soft Imaging Solutions GmbH, Münster, Germany) was then used to demarcate the infarct boundary, defined by a significant loss in LV myocardium tissue and presence of fibrotic tissue (i.e. a thinning in the LV wall ±2 SDs of mean wall thickness), as previously described.[20] Average infarct size (%) was then quantified as the ratio of infarct circumference-to-overall LV circumference.

Contractile function

A fibre bundle from the diaphragm was isolated to allow *in vitro* contractile function to be assessed using a length-controlled lever system (301B, Aurora Scientific Inc., Aurora, Canada), as previously described.[19,22] Briefly, a muscle bundle was mounted vertically in a buffer-filled organ bath (~22 °C), set at optimal length, and after 15 min was stimulated via a force–frequency protocol using 1–300 Hz (600 mA, 500 ms train duration, and 0.25 ms pulse width). The muscle was then subjected to a force–velocity protocol where it was allowed to shorten against external loads (80–10% of the maximal tetanic force; each separated by 1 min) after being stimulated at 150 Hz for 300 ms. Shortening velocity was determined 10 ms after the first change in length and on the linear section of the transient (DMA software, Aurora Scientific Inc.). Force (N) was normalized to muscle cross-sectional area (CSA; cm^2) by dividing muscle mass (g) by the product of L_o (cm) and estimated muscle density (1.06), which allowed specific force in N/cm^2 to be calculated.

DOI: 10.1002/jcsm.12448

Figure 1 An overview of the study design (A). Animals at an age of 12 weeks were either subjected to myocardial infarction to induce chronic heart failure (CHF) or sham operated. One week after myocardial infarction echocardiography was performed to confirm reduced contractility. Animals with a left ventricular ejection fraction (LVEF) <20% were randomized into groups either receiving normal mouse chow (CHF) or chow supplemented with compound ID#704946 (CHF + 704946). Nine weeks after randomization echocardiography was repeated, animals were sacrificed, and tissue was collected for subsequent analysis. Echocardiographic analyses 1 week after sham operation or myocardial infarction and prior randomization revealed a significant reduction in LVEF (B) and fractional shortening (FS) (C) in CHF and CHF + 704946 mice. Representative images of myocardial sections stained with Picosirius red after the treatment period are shown (D) documenting clear fibrosis in the CHF and CHF + 704946 animals. LAD, left anterior descending coronary artery.

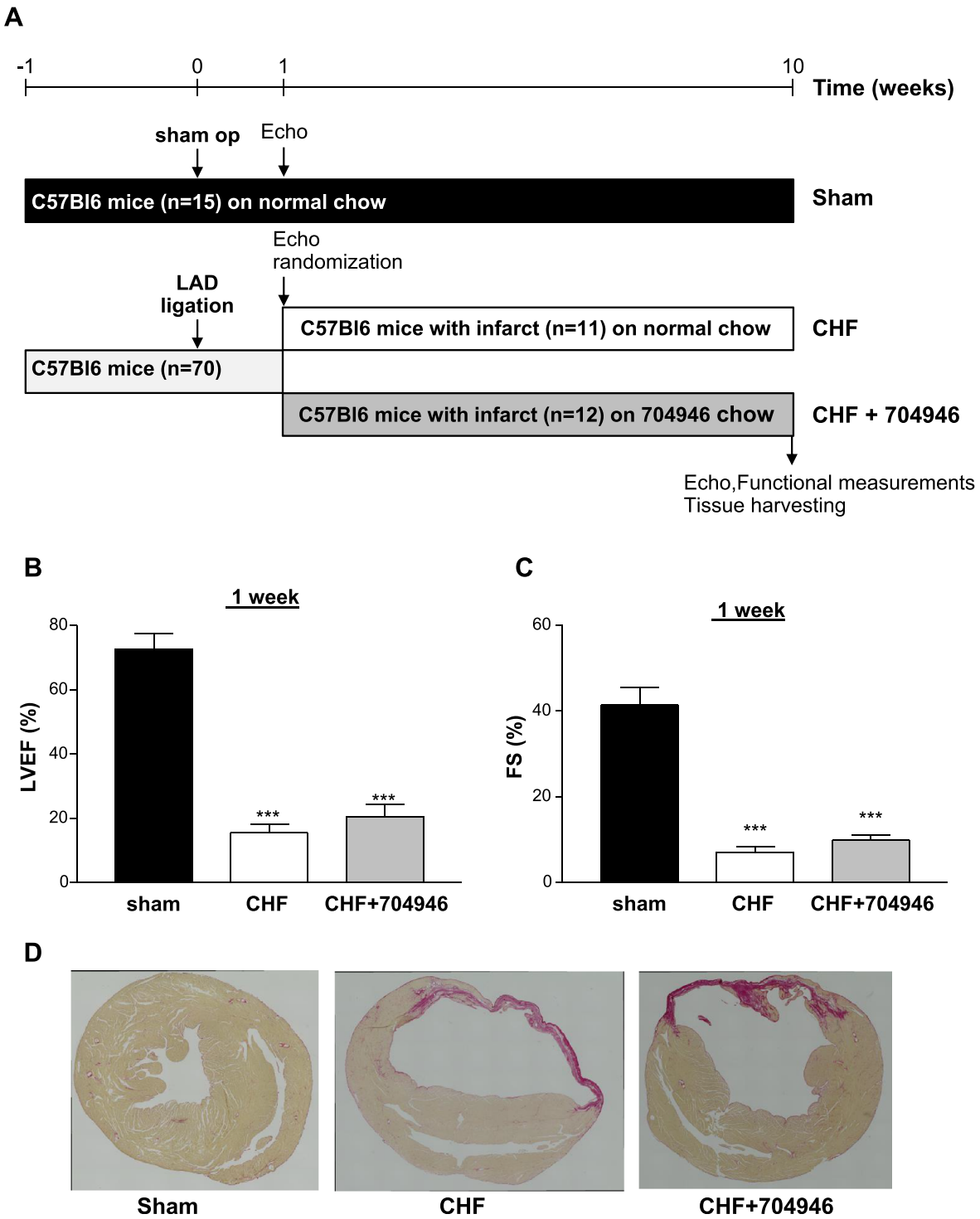

DOI: 10.1002/jcsm.12448

Shortening velocity was normalized to optimal muscle length (in L_o/s), while power was calculated for each load as the product of shortening velocity and specific force (in W/cm^2).

Diaphragm analyses

Paraffin-embedded diaphragm sections (3 μm) were stained with periodic acid–Schiff, and fibre CSA was subsequently evaluated by imaging software (ImageJ, open source software). For quantification of fibre-type distribution, paraffin sections (3 μm) were incubated for 1 h after antigen retrieval with a primary antibody to slow myosin heavy chain (1/75 dilution, Abcam, Cambridge, UK). After extensive washing with PBS, the sections were incubated with an anti-mouse peroxidase secondary antibody (1 h, Sigma, Taufkirchen, Germany, 1:250), followed by AEC (3-amino-9-ethylcarbazole) staining. Positive-stained (type I fibres) and negative-stained fibres (type II fibres) were counted by image analysis software (ImageJ), and per cent distribution was calculated.

Proteomic and western blot analysis

Mass spectrometry-based proteomic analysis was performed at the DZHK Core Facility, Bad Nauheim, Germany (see details in the Supporting Information). Obtained MS raw data were processed by MaxQuant (1.6.0.1)[23] using the Andromeda search engine and the Uniprot database for Mus musculus (as of 20 April 2017). At a false discovery rate of 1%[24] (both peptide and protein levels; see also Supporting Information, *Figure S1*), >2600 protein groups were identified. The reductive dimethylation protocol employed[25] yielded pairwise relative comparative quantitation (ratios) between proteins from CHF + 704946, CHF, and sham conditions, which were statistically queried for significant differences (see details in the Supporting Information). Selected polypeptides detected as significantly changing were validated using western blotting.

For western blot analyses, frozen diaphragm was homogenized in relaxing buffer (90 mmol/L HEPES, 126 mmol/L potassium chloride, 36 mmol/L sodium chloride, 1 mmol/L magnesium chloride, 50 mmol/L EGTA, 8 mmol/L ATP, and 10 mmol/L creatine phosphate, pH 7.4) containing a protease inhibitor mix (Inhibitor Mix M, Serva, Heidelberg, Germany) and sonicated. Protein concentration of the supernatant was determined (bicinchoninic acid assay, Pierce, Bonn, Germany), and aliquots (5–20 μg) were separated by sodium dodecyl sulfate–polyacrylamide gel electrophoresis. Proteins were transferred to a polyvinylidene fluoride membrane and incubated overnight at 4 °C using the following primary antibodies: porin and telethonin (both 1/1000, Abcam, Cambridge, UK), MRPS-5 (1/500, Thermo Fisher, Rockford, IL, USA), MuRF1 and MuRF2 (both 1/1000; raised in the Labeit laboratory[26] and also commercially available from Myomedix, Neckargemünd, Germany), and Tom20 (1:200, Santa Cruz Biotechnologies, Heidelberg, Germany). Membranes were subsequently incubated with a horseradish peroxidase-conjugated secondary antibody, specific bands were visualized by enzymatic chemiluminescence (Super Signal West Pico, Thermo Fisher Scientific Inc., Bonn, Germany), and densitometry was quantified using a one-dimensional scan software package (Scanalytics Inc., Rockville, MD, USA). Measurements were normalized to the loading control GAPDH (1/30 000; HyTest Ltd, Turku, Finland) or α-tubulin (1:1000, Santa Cruz Biotechnologies). All data are presented as fold change relative to sham.

Enzyme activity measurements

Diaphragmatic tissue was homogenized in relaxing buffer, and aliquots were used for enzyme activity measurements. Enzyme activities for lactate dehydrogenase (EC 1.1.1.27), pyruvate kinase (EC 2.7.1.40), succinate dehydrogenase (SDH, EC 1.3.5.1), citrate synthase (CS, EC 2.3.3.1), β-hydroxyacyl-COA dehydrogenase (EC 1.1.1.35), and mitochondrial complex I were measured spectrophotometrically as previously described in detail.[27–31] Enzyme activity data are presented as the fold change relative to sham.

Differential scanning fluorimetry analysis

'MuRF1 central' fragment was expressed as previously described[32] and used in differential scanning fluorimetry (DSF) experiments at 75 μmol/L final concentration. Compound ID#704946 was diluted from a 10 mmol/L stock in DMSO to 100 μmol/L in PBS as DSF assay buffer, resulting in a final concentration of 1% DMSO. After 1 h pre-incubation at room temperature, the aqueous protein solutions were soaked into capillaries and placed into a Prometheus NT.48 nanoDSF device (NanoTemper Technologies, Munich, Germany). Changes in the intrinsic tryptophan or tyrosine fluorescence that occurred after light-emitting diode laser excitement upon protein unfolding in a thermal gradient were detected at 330 and 350 nm, respectively.

Cell culture, reverse transcription PCR, and transcriptome analysis

C2C12 myotubes[19] were incubated with or without compound ID#704946 for 20 min at a final concentration of 10 μmol/L. After the incubation period, total RNA was isolated (miRNeasy Mini Kit, Qiagen, Hilden, Germany) and reverse transcribed into cDNA (Revert AIDTM H Minus First Strand Synthesis Kit, Thermo Fisher Scientific Inc.) using

oligo-dT primers. Real-time PCR was performed using the CFX96TM or CFX384TM Real-Time PCR System (Bio-Rad, Hercules, CA, USA) and Maxima SYBR Green qPCR Kit (Thermo Fisher Scientific Inc.). Primers used for real-time–reverse transcription PCR analysis are listed in Supporting Information, *Table* S1. Relative quantification of gene expression was calculated by CT method with Polr2a and Tbp as housekeeping genes as recently described.[33]

Transcriptome analysis was performed as briefly outlined. Barcoded stranded mRNA sequence libraries were prepared from high-quality total RNA samples (~200 ng per sample) using the Illumina TruSeq RNA Sample Preparation v2 Kit (Illumina, San Diego, CA, USA) implemented on the liquid handling robot Beckman FXP2. Obtained libraries were pooled in equimolar amounts; 1.8 pmol/L solution of this pool was loaded on the Illumina sequencer NextSeq 500 and sequenced unidirectionally, generating ~500 million reads, each 85 bases long. Base calling of the sequencing run was performed using bcl2fastq v2.20 (Illumina, San Diego, CA, USA).

Table 1 Animal characteristics after 10 weeks of intervention

	Sham (n = 15)	CHF (n = 11)	CHF + 704946 (n = 12)
Physical			
Body weight (g)	22.6 ± 0.5	22.4 ± 0.6	23.8 ± 0.4
Heart-to-body weight (g/mg)	5.03 ± 0.11	7.87 ± 0.55***	7.52 ± 0.57***
Lung weight (wet/dry)	4.16 ± 0.07	4.48 ± 0.06*	4.47 ± 0.10*
Histology			
LV infarct size (%)	—	30.5 ± 4.6	27.1 ± 2.9
Echocardiography			
LVEDD (mm)	3.8 ± 0.1	6.2 ± 0.2***	5.9 ± 0.2***
LVESD (mm)	2.6 ± 0.1	5.8 ± 0.3***	5.3 ± 0.2***
LVEF (%)	59.6 ± 2.7	16.1 ± 2.9***	21.1 ± 2.5***
LVFS (%)	31.8 ± 1.9	7.5 ± 1.4***	9.9 ± 1.2***

CHF, chronic heart failure; LV, left ventricle; LVEDD, left ventricular end-diastolic diameter; LVEF, left ventricular ejection fraction; LVESD, left ventricular end-systolic diameter; LVFS, left ventricular fractional shortening.
Data are presented as mean ± standard error of the mean.
*$P < 0.05$ vs. sham.
***$P < 0.001$ vs. sham.

Figure 2 *In vitro* contractile function of diaphragm fibre bundles, as assessed during isometric (A, B) and isotonic contractions (C, D). Comparing maximal specific force (B) and maximal power (D), chronic heart failure (CHF) animals demonstrated a 21 and 28% reduction, respectively, which was significantly attenuated by ID#704948. Data are presented as mean ± standard error of the mean. $^{*}P < 0.05$, $^{**}P < 0.01$, $^{***}P < 0.001$ vs. CHF, $^{\S}P < 0.05$, and $^{\S\S}P < 0.01$ vs. CHF + 704946.

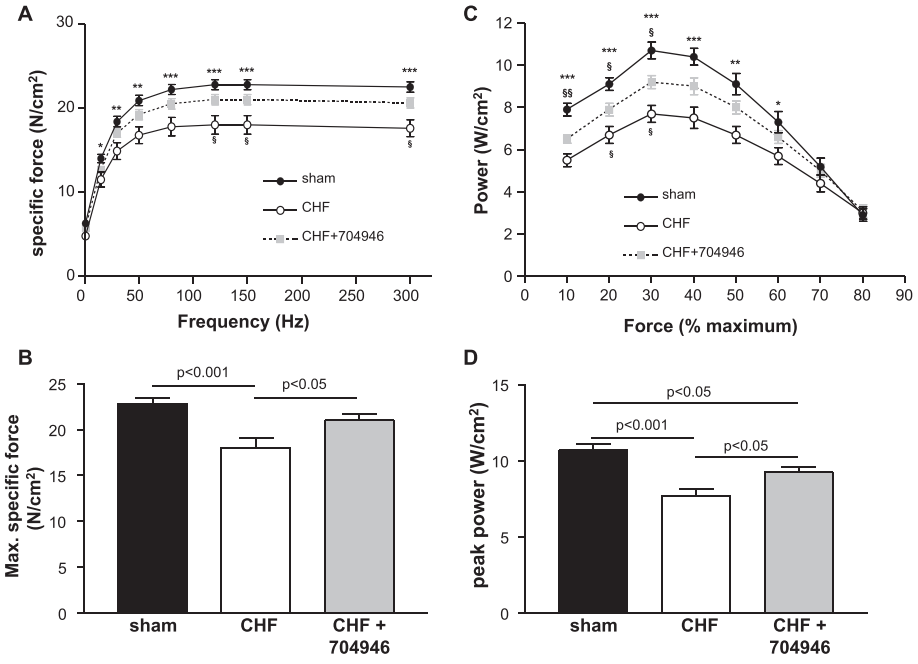

DOI: 10.1002/jcsm.12448

Sequencing reads were aligned onto Mus musculus genome reference (GRCm38.p6-mm10) with STAR aligner.[34] Read counting was performed using the STAR's in-built implementation of HTSeq-count.[35] Transcriptomic analysis was carried out using the DESeq2 v1.22.2 package.[36]

Statistical analyses

Data are presented as mean ± standard error of the mean. One-way analysis of variance followed by Bonferroni *post hoc* was used to compare groups, while two-way repeated measures analysis of variance followed by Bonferroni *post hoc* was used to assess contractile function (GraphPad Prism). Significance was accepted as $P < 0.05$.

Results

Mouse model of chronic heart failure

One week post-MI, 23 out of 70 LAD-ligated mice (32%) exhibited a significant impairment of cardiac function, as evidenced by an ~75% reduction in LVEF (*Figure* 1B) and ~72% reduction in LVFS (*Figure* 1C) as compared with sham. These mice were randomly assigned to two different groups, receiving either control or compound ID#704946-supplemented diet for 9 weeks. Compared with sham mice at 10 weeks, MI-induced mice developed typical signs of CHF, as evidenced by pulmonary congestion (i.e. increased lung weight) and greater cardiac mass (*Table* 1). In addition, echocardiography revealed an enlarged left ventricle (significant increase LVEDD and LVESD) and impaired LV function (reduction in LVEF and LVFS) (*Table* 1). Mean infarct size was ~30% (*Figure* 1). No significant differences in lung or cardiac parameters were detected between compound ID#704946-treated and non-treated CHF animals, suggesting groups were well matched in terms of disease severity.

Chronic heart failure-induced diaphragm myopathy

Compared with sham animals, mice with CHF on control chow developed a diaphragm myopathy at week 10: significant muscle weakness in the diaphragm was demonstrated across a range of stimulation frequencies (*Figure* 2A), with maximal force reduced by 21% (*Figure* 2B). An impairment between sham and CHF animals was also apparent from power

Figure 3 Cross-sectional area (A, B) and fibre-type distribution (C, D) was evaluated in diaphragm sections from all three groups. Paraffin sections of the diaphragm were stained with periodic acid–Schiff (A), and the cross-sectional area was determined by ImageJ (B). The distribution of type I and type II was quantified in diaphragm samples from all three groups, after staining paraffin sections with a myosin heavy chain slow isoform antibody (dark brown fibres = type I fibres; non-stained fibres = type II fibres) (D). Data are presented as mean ± standard error of the mean. CHF, chronic heart failure.

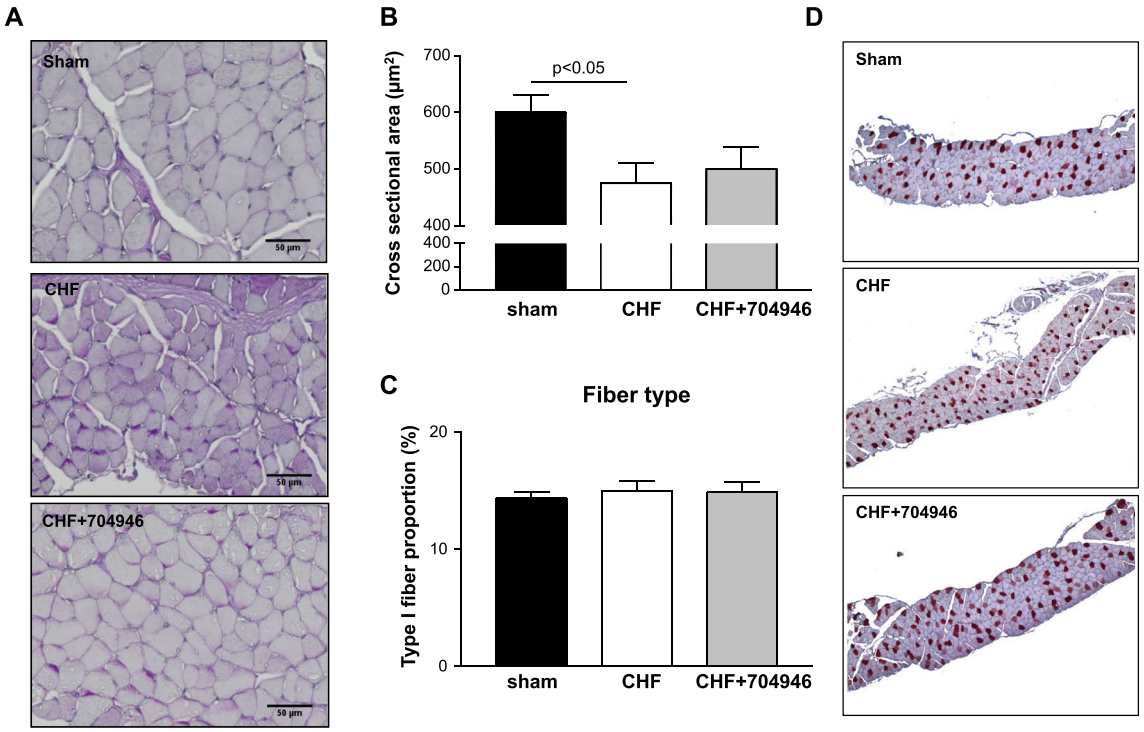

DOI: 10.1002/jcsm.12448

generation measured in fibre bundles (*Figure* 2C), with peak power reduced by 28% (*Figure* 2D). This muscle dysfunction was accompanied by muscle atrophy, as evidenced by a 21% reduction in fibre CSA in CHF (*Figure* 3A and 3B).

Feeding with compound ID#704946 attenuates diaphragm myopathy in chronic heart failure

Consistent with our previous report,[19] feeding of compound ID#704946 was well tolerated by the mice, and food intake did not change (data not shown). Compound feeding resulted in significant contractile benefits to the diaphragm: maximal force (*Figure* 2A and 2B) and peak power (*Figure* 2C and 2D) were improved, while fibre atrophy was only slightly but not significantly improved (*Figure* 3A and 3B). No difference in skeletal muscle fibre type I proportion was evident between the three groups (*Figure* 3C and 3D).

Proteome analyses

To generate hypotheses on the molecular mechanisms underlying the observed physiological changes and benefits, we next performed comparative quantitative proteomic analysis of diaphragm tissue from sham, CHF, and CHF + compound-treated mice. Using standard statistical tests, several proteins were identified to be statistically different (e.g. TNNT3, Timm9, Ccdc5, Adi1, Ptges3, and Ndufa3). After applying multiple hypothesis testing (Benjamini–Hochberg; corrected $P < 0.05$) for comparison of CHF mice with and without compound feeding, only Mrps5 (mitochondrial ribosomal protein 5) remained as a significantly up-regulated protein ($P = 0.02$; *Figure* 4A). This finding is reinforced by the fact that the protein is also found significantly enriched in the CHF + compound vs. sham comparison. Western blotting was used to confirm this difference in all animals used in the study (*Figure* 4B), and as a result, mitochondrial dysfunction was hypothesized to be involved in CHF-induced myopathy.

Compound ID#704946 treatment normalizes mitochondrial metabolism and MuRF2 expression

Because proteomic profiling data generated the hypothesis of an impaired mitochondrial homeostasis, we proceeded with measuring enzymatic activities of key mitochondrial enzymes. Measuring specific enzyme activity of mitochondrial enzymes including CS (*Figure* 5A), SDH (*Figure* 5B), and mitochondrial complex I (*Figure* 5C) revealed a significant reduction by 21, 28, and 27%, respectively, in the diaphragm of CHF animals when compared with sham. No difference was noted for creatine kinase (*Figure* 5D). The amount of mitochondria in diaphragm tissue, as assessed by the protein expression of the

Figure 4 Diaphragm tissues from mice sacrificed after completion of the myocardial infarction-compound feeding intervention study was characterized by mass spectrometry-based quantitative proteomics analysis. (A) Mrps5, a mitochondrial-cytosolic shuttle protein in charge of protein initiation and elongation in the mitochondrial ribosome, is decreased significantly in the chronic heart failure (CHF) group in comparison with both the sham + compound control group and the CHF + compound group, respectively. Each data point represents protein ratio data between two mice. Relative changes in protein ratio are shown on the *y*-axis as log2. By Bayesian moderated *t*-testing as implemented in the R package limma and after multiple hypothesis testing correction (Benjamini–Hochberg), corrected *P* values are 0.02 for CHF + compound vs. CHF or for sham + compound vs. CHF. Proteins with $P < 0.05$ before Benjamini–Hochberg correction were not included at this stage. (B) Western blot analysis was performed for Mrps5 in the diaphragm of all animals included into the study. A significant reduction of Mrps5 expression was noted in CHF, which was reversed by compound ID#704946 feeding. A representative western blot is shown, and data are presented as mean ± standard error of the mean.

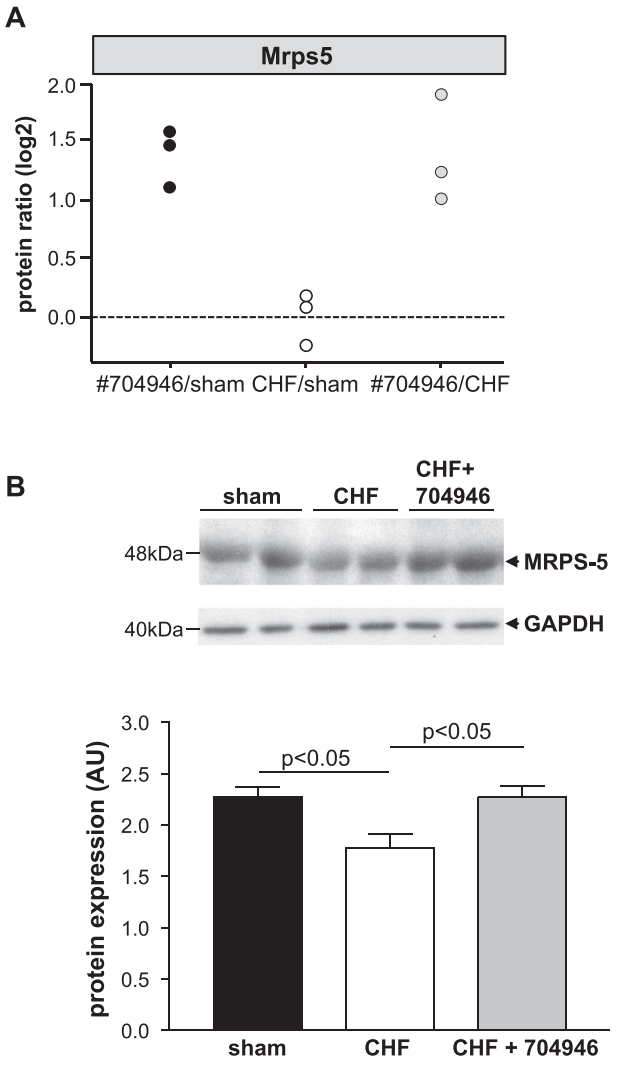

Figure 5 Enzyme activities of citrate synthase (A), succinate dehydrogenase (B), mitochondrial complex I (C), and creatine kinase (D). In addition, protein expression of mitochondrial porin of the outer mitochondrial membrane (E) and TOM-20 (F) was quantified in diaphragm samples from all animals in the three groups [sham, chronic heart failure (CHF), and CHF + 704946]. A representative western blot for the detection of porin, TOM-20, and GAPDH is shown (G). Our data revealed a significant down-regulation of citrate synthase and succinate dehydrogenase activity and porin and TOM-20 expression in CHF when compared with sham, but this was attenuated in mice fed the compound ID#704946. No difference in creatine kinase activity was observed between the three groups. Data are presented as mean ± standard error of the mean.

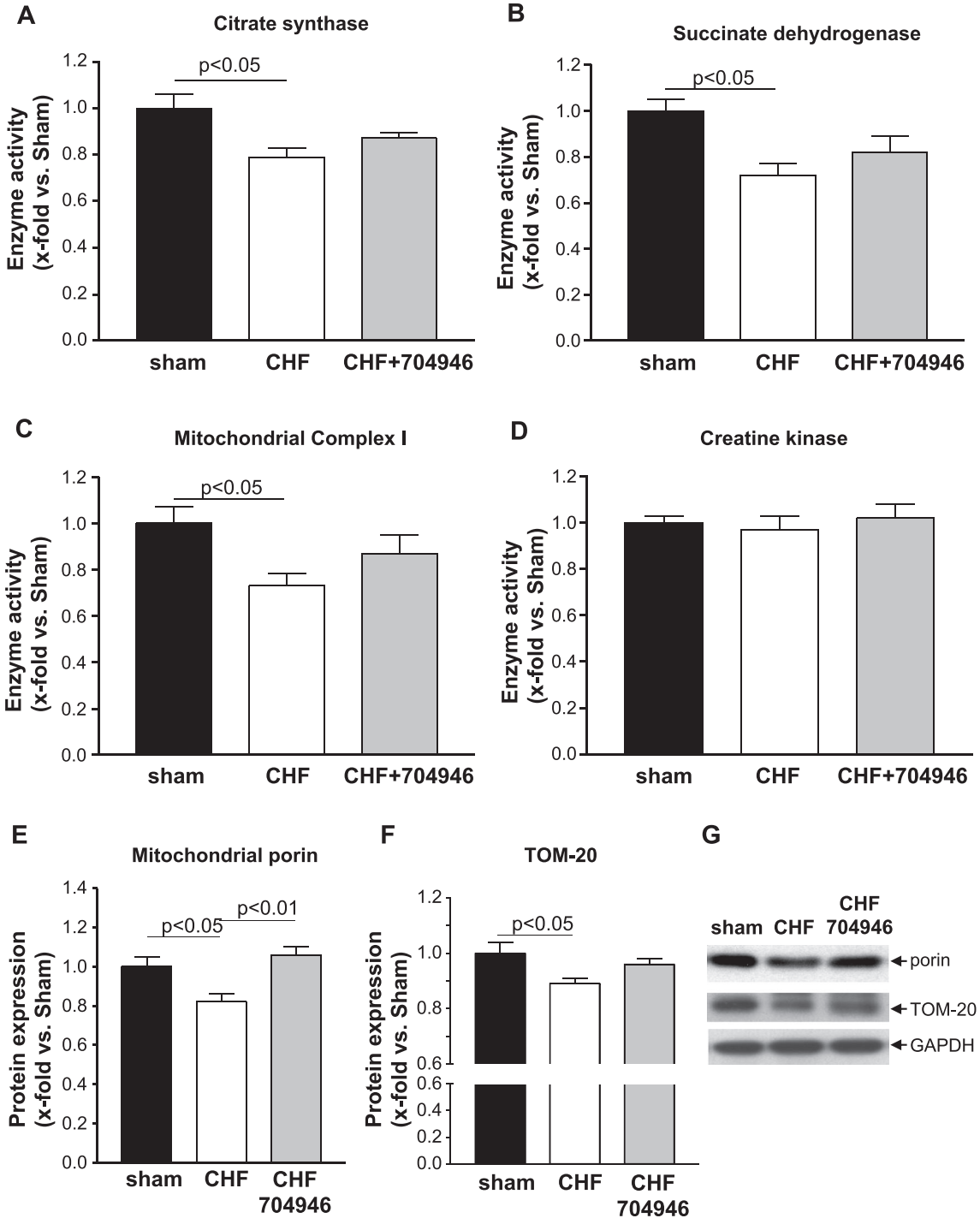

DOI: 10.1002/jcsm.12448

mitochondrial porin expression (*Figure* 5E) and TOM-20 (*Figure* 5F), was also significantly reduced in CHF mice. Consistent with effects on mitochrondrial functions, treatment with compound ID#704946 partially improved CS, SDH, and mitochondrial complex I enzyme activity (*Figure* 5A–C) and resulted in near-normal porin and a modest, but statistically significant, improvement in TOM-20 expression (*Figure* 5E and 5F). In contrast, when assessing cytoplasmic enzymes for glycolysis and fatty acid metabolism (glycolysis: pyruvate kinase and lactate dehydrogenase; fatty acid metabolism: β-hydroxyacyl-COA dehydrogenase), no difference was detected between the three groups (*Figure* 6A–C). We further evaluated how the expression of MuRF1 and MuRF2, an isoform of MuRF1, responded to the development of CHF and feeding with compound ID#704946. MuRF1 and MuRF2 expression was significantly up-regulated in the CHF group (*Figure* 7A and 7B), and this was prevented by treatment with compound ID#704946 (*Figure* 7A and 7B). Quantifying the expression of telethonin, a MuRF1 target protein, a trend (P = 0.08) towards a reduced expression in the CHF group was observed, which was not evident in the compound ID#704946-treated group (*Figure* 7C).

Figure 6 Enzyme activities of lactate dehydrogenase (A), pyruvate kinase (B), and β-hydroxyacyl-COA dehydrogenase (C) were quantified in diaphragm samples from all animals in the three groups [sham, chronic heart failure (CHF), and CHF + 704946]. No difference for these enzymes was observed between the three groups. Data are presented as mean ± standard error of the mean.

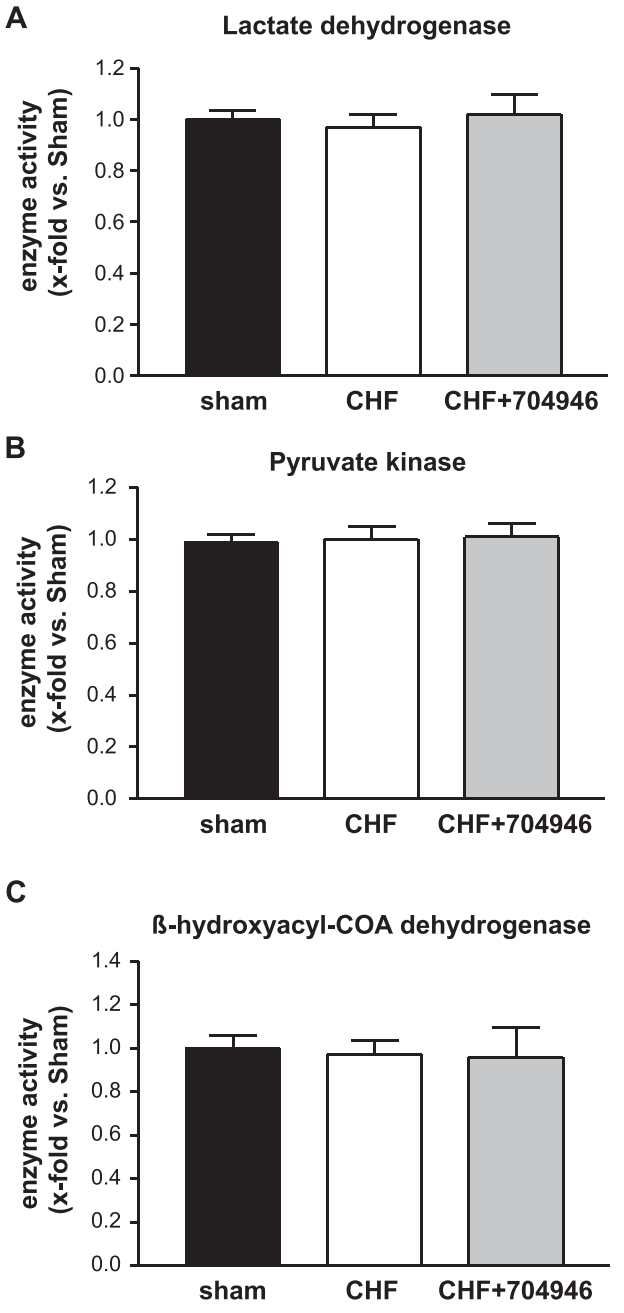

Treatment of myotubes with compound ID#704946

Transcriptome analysis of C2C12 myotubes treated for 20 min with compound ID#704946 was performed by real-time–reverse transcription PCR and next-generation sequencing. Analysing the expression of pre-specified genes (MafBx, MuRF1 and MuRF2, Tom20, and porin) detected only small minor changes (4–10% reduction by compound ID#704946) (Supporting Information, *Figure* S2). Running unbiased next-generation sequencing of the samples revealed that out of 16 383 genes in the reference, 13% (2165 genes) did not have enough read counts to be part of the analysis (mean count of reads across samples was <1). No genes were identified as outliers, and 87 genes (0.53%) were found differentially expressed between control and treatment but with relative small changes (log2 fold change $<\pm1$). Out of the 87genes, 63 had higher expression in the treated samples, and 24 had lower expression in the treated samples. For a detailed view of the altered genes, see Supporting Information, *Table* S2.

Differential scanning fluorimetry analysis

In vitro, compound ID#704946 significantly lowers the melting temperature of 'MuRF1 central', as indicated by DSF (*Figure* 8). The first derivative of the fluorescence wavelength ratio of 350/330 nm upon thermal protein unfolding was used to calculate transition midpoint (Tm) of single and multiple transition states. Tm of MuRF1 central in PBS was 65.2 °C and was only negligible changed to 65.8 °C by the addition of 1% DMSO. In contrast, a strong effect on the thermal unfolding of MuRF1 was observed by the addition of compound ID#704946. Compound ID#704946 destabilized MuRF1 as indicated by the significantly reduced main Tm of 52.5 °C.

Figure 7 Protein expression of MuRF1 (A), MuRF2 (B), and telethonin (C) was quantified by western blot analysis. MuRF1 and MuRF2 were significantly up-regulated in the chronic heart failure (CHF) group (A, B), which was attenuated in the CHF-704946 group. A bigger effect of compound ID#704946 was seen for MuRF2 when compared with MuRF1. For telethonin expression, a trend towards lower expression was evident in the CHF group, which was attenuated after compound feeding (C) Data are presented as mean ± standard error of the mean.

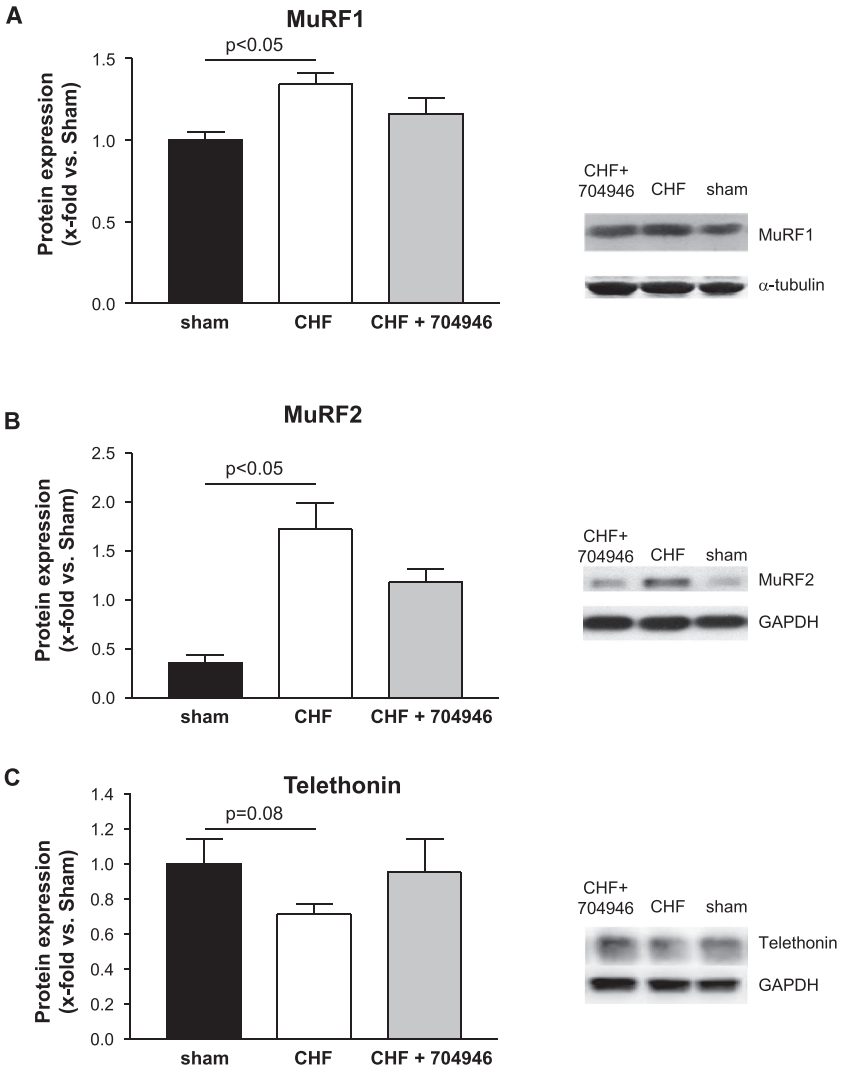

Discussion

It is well established that the development of CHF in patients is associated with skeletal muscle atrophy and dysfunction, which contributes to exercise intolerance and dyspnoea.[19,20,22,37–39] A decline in force generation of ~20% in the diaphragm is apparent as soon as 72 h post-MI,[20] approaching the magnitude observed in end-stage CHF.[22] Studies on patient biopsies and on murine models suggest that the underlying mechanisms are complex and include an activation of the UPS, autophagy, inflammatory response, and apoptosis (for review[40–42]). In this multivariate interplay, induction of MuRF1/MuRF2 has, however, been recognized as an important step, in particular for fibre atrophy and dysfunction.[43,44] In the present study, we thus tested the potential therapeutic benefit of the recently described MuRF1 inhibitor compound ID#704946[19] in a clinically relevant model of CHF, and the results of the study can be summarized as follows:

i The development of CHF is associated with diaphragm atrophy and dysfunction, which is significantly reversed by compound ID#704946.
ii Enzymes involved in mitochondrial energy production and mitochondrial homeostasis were significantly impaired in diaphragm tissue during CHF, whereas treatment with compound ID#704946 essentially normalized their activity/expression.

Figure 8 The effect of compound ID#704946 on MuRF1 protein stability was determined *in vitro* by differential scanning fluorimetry. Changes in the intrinsic protein fluorescence in a thermal gradient were monitored at 350 and 330 nm, respectively. The first derivative of the fluorescence wavelength ratio of 350/330 nm upon thermal protein unfolding was used to calculate transition midpoint (Tm) of single and multiple transition states. Tm of MuRF1 central in phosphate-buffered saline (solid line) was 65.2 °C and was only negligible changed to 65.8 °C by the addition of 1% DMSO (dashed line). In contrast, a strong effect on the thermal unfolding of MuRF1 was observed by the addition of compound ID#704946 (dotted line). Compound ID#704946 destabilized MuRF1 as indicated by the significantly reduced main Tm of 52.5 °C.

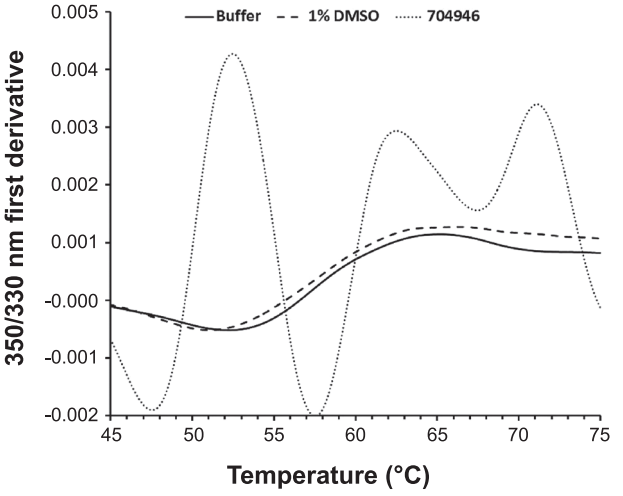

iii Feeding with compound ID#704946 had no apparent undesired side effects such as on the reduced cardiac contractility and myocardial hypertrophy response in this murine heart failure model.

Treatment of diaphragm dysfunction and atrophy by compound ID#704946

Diaphragmatic weakness of 15–20% as reported for heart failure in the present study is comparable with other diseases like mechanical ventilation and sepsis,[45,46] critically ill patients,[47] or pulmonary hypertension[48] and is reported to be of clinical relevance with respect to mortality.[49] In the present study, we tested the effects of compound ID#704946 when fed to animals 7 days after the MI for 9 weeks as a secondary prevention. Earlier observations from our group documented that 3 days post-MI diaphragmatic function is significantly impaired.[20] Intriguingly, in the present secondary prevention setting, compound ID#704946 reversed diaphragm function to nearly normal values without big effects on muscle mass. This is in contrast to observations made earlier in a cardiac cachexia model where an effect of compound ID#704946 was seen on function and muscle mass.[19] This possibly relates to a diversity of underlying mechanisms, length of intervention, or pharmacokinetics, but further studies are necessary to address this in more detail. Other approaches to counteract muscle atrophy in different models of wasting conditions have been recently described and include administration of β-hydroxy β-methylbutyrate (HMB),[50] 1,25-dihydroxyvitamin D,[51] anti-interleukin-6 antibody treatment,[51] IκB kinase-β inhibition by IMD-0354,[52] or direct inhibition of the UPS by MG132.[53–55] In the majority of these studies, however, the pharmacological agent was administered prior to initiating muscle atrophy by hindlimb suspension[51] or did not prevent muscle atrophy.[52] The use of MG132 is discussed controversially with a subset of studies reporting positive effects on muscle atrophy induced by hindlimb unloading,[53,55] or tumour,[54] whereas others saw no effects.[56,57] Importantly, when assessing the impact of MG132 on muscle force, no positive effect was obvious.[56] This is in clear contrast to compound ID#704946 treatment, where improved fibre contractility was evident. Taken together, the chemical knock-down of MuRF1 and MuRF2 by compound ID#704946 appears a viable treatment strategy to follow up on the amelioration of diaphragm dysfunction in cardiac failure. Previous studies on MuRF1 knockout mice suggested an increased vulnerability for cardiac hypertrophy during pressure overload.[58] It is of note that in the present study, no exaggerated cardiac hypertrophic response was evident when feeding compound ID#704946 during the development of CHF, an observation that nevertheless requires validation in additional studies on non-stressed animals.

Potential underlying mechanisms

The molecular analyses performed in the present study suggest that a decay of mitochondrial function is involved in CHF-induced muscle dysfunction and that compound ID#704946 is able to rescue mitochondrial impairment. Comparing protein expression by quantitative proteomic analysis and follow-up for specific mitochondrial enzyme activities confirmed diminished mitochondrial energy production and homeostasis in CHF as reversed by treatment with compound ID#704946. In particular, Mrps5 was the protein with the highest significant induction by compound ID#704946, which was confirmed by conventional western blot analysis. Mrps5, a member of the family of mitochondrial ribosomal proteins, was first described in *Caenorhabditis elegans*, where it was causally involved in regulating lifespan.[59] Knock-down of Mrps5 resulted in reduced mitochondrial respiration, and the worms displayed reduced ATP levels and CS activity.[59] Consistent with this, we detected a clear reduction of mitochondrial complex I activity, which was reversed by compound ID#704946 treatment. The essential role of mitochondrial dysfunction in the pathology of

muscle atrophy is described in many muscle atrophy models including disuse, diabetes, ageing, and CHF.[39,60–62] In the context of CHF-induced diaphragm weakness, a pivotal involvement is further supported by the observation that reduction of mitochondrial reactive oxygen species by MitoTEMPO counteracted the dysfunction.[63]

The exact molecular mechanism by which compound ID#704946 exerts these beneficial effects on the mitochondria remains to be determined, as this compound was originally identified as an inhibitor of the interaction between the MuRF1 and the giant myofibrillar protein titin. Our DSF results suggest a destabilization of MuRF1's coiled-coil region caused by compound ID#704946 *in vitro*. With regard to signalling effects caused by compound ID#704946 during feeding *in vivo*, future studies are required to determine if MuRF1 destabilization occurs also *in vivo* (possibly accounting for the modest reduction of MuRF1 steady-state expression levels) or if binding of compound ID#704946 to MuRF1's central region attenuates target recognition (possibly inhibiting binding to titin and/or increasing myocellular telethonin levels, see the succeeding texts). Previous studies on the cellular interacting partners of MuRF1 identified numerous myofibrillar proteins and also many genes involved in mitochondrial biology and energy metabolism.[64] Consistent with this, transgenic overexpression of MuRF1 in skeletal muscle shows perturbed carbohydrate metabolism and glucose tolerance in mice.[26] Therefore, we previously speculated that an induction of MuRF1 in the skeletal muscles during chronic stress (e.g. CHF[65,66]) may trigger MuRF1 to ubiquitinate nuclear-encoded proteins of the mitochondrial respiratory chain during their cytoplasmic transport to the mitochondria in an effort to conserve energy metabolites. Accordingly, treatment by compound ID#704946 could reverse this detrimental effect in chronic stress states where MuRF1 acts as a negative regulator of mitochondrial energy production. In accordance with this hypothesis and our previous report,[19] a significant up-regulated MuRF1 expression was evident in CHF, which was blunted by compound ID#704946. In line with the effect of compound ID#704946 on MuRF1 expression, also a trend towards a reduced expression of telethonin, a known substrate for MuRF1,[67,68] was seen in CHF, which was also blunted in the compound-treated group. To our surprise, we also detected a significant modulation of MuRF2 by compound ID#704946. A possible explanation why compound ID#704946 also attenuates MuRF2 induction is that the recombinant MuRF1 fragment, which was used to fish compound ID#704946 from the in-house EMBL compound collection, corresponds to its central coiled-coil domain (MuRF1cc) that is highly conserved between MuRF1 and MuRF2.[67] Therefore, compound ID#704946 may act on both MuRF1 and MuRF2, and studies are ongoing to determine this. Future studies are also required to determine if the modest reduction of MuRF1 expression in the compound ID#704946-treated group, or rather an attenuated interaction of MuRF1 with its target proteins, or mechanisms unrelated to both underlie its protective effects. Furthermore, preliminary high-performance liquid chromatography–mass spectrometry studies indicated after intraperitoneal or oral delivery a rapid appearance in serum, followed by a fast metabolization. Therefore, additional studies are mandatory to determine the metabolism and bioavailability of compound ID#704946.

Study limitations

An important principal limitation of our study is the relevance of the used murine model for human heart failure: the underlying mechanisms may principally differ between human and mice, but in this study, we tried to control for this by following CHF closely by echocardiography and selecting mice as appropriate to mimic the human condition. Another limitation is that the used compound is unrelated to other known drugs. Presently, no pharmacological data or data on toxicity, pharmacokinetics, and bioavailability are available. As such, follow-up studies are needed to determine if compound ID#704946 indeed can be a future drug candidate.

Acknowledgements

Mass spectrometry parts of this study were supported by the DZHK project 'Tititn mass spec', column B tandem Mannheim–Bad Nauheim. The authors certify that they comply with the ethical guidelines for authorship and publishing in the *Journal of Cachexia, Sarcopenia, and Muscle*.[69]

This article is devoted in memoriam to Dittmar Labeit - we all miss him.

Conflict of interest

Patent pending for compound ID#704946 and its application to chronic muscle stress states.

Funding

We are grateful to the Fondation Leducq (network 13CVD04) for generous support, to the European Union Horizon 2020 research and innovation programme (grant agreement no. 645648 'Muscle Stress Relief'), to the AFBS (a foundation for Building Strength; http://buildingstrength.org), and to the Wilhelm Müller Stiftung Mannheim (founded by Ruth Müller).

Online supplementary material

Additional supporting information may be found online in the Supporting Information section at the end of the article.

Figure S1: Overview of protein ratio distributions given as log2 in the different triplicate samples (R1-3). Here 'MI' indicates myocardial infarction, 'Ctrl' sham and 'B4' compound treatment after myocardial infarction. 'Mi_Ctrl' encodes the relative protein ration of mycardial infarction over on.

Figure S2: mRNA expression of MafBx (A), MuRF1 (B), MuRF2 (C), Tom20 (D) and porin (E) was analyzed in C2C12 myotubes incubated without (con) or with 10 μM #704946 for 20 min by qRT-PCR. Values are expressed as fold changes vs. control.

Table S1: Primer Sequences

Table S2: List of genes significantly altered by ID#704946

References

1. Wannamethee GS, Shaper AG, Lennon L, Whincup PH. Decreased muscle mass and increased central adiposity are independently related to mortality in older men. *Am J Clin Nutr* 2007;**86**:1339–1346.
2. Rantanen T, Harris T, Leveille SG, Visser M, Foley D, Masaki K, et al. Muscle strength and body mass index as long-term predictors of mortality in initially healthy men. *J Gerontol A Biol Sci Med Sci* 2018;**55**: M168–M173.
3. Martin L, Birdsell L, MacDonald N, Reiman T, Clandinin MT, McCargar LJ, et al. Cancer cachexia in the age of obesity: skeletal muscle depletion is a powerful prognostic factor, independent of body mass index. *J Clin Oncol* 2013;**31**:1539–1547.
4. Fülster S, Tacke M, Sandek A, Ebner N, Tschöpe C, Doehner W, et al. Muscle wasting in patients with chronic heart failure: results from the studies investigating co-morbidities aggravating heart failure (SICA-HF). *Eur Heart J* 2013;**34**:512–519.
5. Lecker SH, Solomon V, Mitch WE, Goldberg AL. Muscle protein breakdown and the critical role of the ubiquitin–proteasome pathway in normal and disease states. *J Nutr* 1999;**129**:227S.
6. Lecker SH, Jagoe RT, Gilbert A, Gomes M, Baracos VE, Bailey J, et al. Multiple types of skeletal muscle atrophy involve a common program of changes in gene expression. *FASEB J* 2004;**18**:39–51.
7. Sandri M. Protein breakdown in muscle wasting: role of autophagy–lysosome and ubiquitin–proteasome. *Int J Biochem Cell Biol* 2013;**45**:2121–2129.
8. Cohen S, Brault JJ, Gygi SP, Glass DJ, Valenzuela DM, Gartner C, et al. During muscle atrophy, thick, but not thin, filament components are degraded by MuRF1-dependent ubiquitylation. *J Cell Biol* 2009;**185**.
9. Cohen S, Nathan JA, Goldberg AL. Muscle wasting in disease: molecular mechanisms and promising therapies. *Nat Rev Drug Discov* 2014;**14**:58–74.
10. Attaix D, Ventadour S, Codran A, Bechet D, Taillandier D, Combaret L. The ubiquitin–proteasome system and skeletal muscle wasting. *Essays Biochem* 2005;**41**:173–186.
11. Adams V, Mangner N, Gasch A, Krohne C, Gielen S, Hirner S, et al. Induction of MuRF1 is essential for TNF-α-induced loss of muscle function in mice. *J Mol Biol* 2008;**384**:48–59.
12. Bodine SC, Latres E, Baumhueter S, Lai VKM, Nunez L, Clarke BA, et al. Identification of ubiquitin ligases required for skeletal muscle atrophy. *Science* 2001;**294**: 1704–1708.
13. Li YP, Chen Y, Li AS, Reid MB. Hydrogen peroxide stimulates ubiquitin-conjugating activity and expression of genes for specific E2 and E3 proteins in skeletal muscle myotubes. *Am J Physiol Cell Physiol* 2003;**285**:C806–C812.
14. Baehr LM, Furlow JD, Bodine SC. Muscle sparing in muscle RING finger 1 null mice: response to synthetic glucocorticoids. *J Physiol* 2011;**589**:4759–4776.
15. Eddins MJ, Marblestone JG, Suresh Kumar KG, Leach CA, Sterner DE, Mattern MR, et al. Targeting the ubiquitin E3 ligase MuRF1 to inhibit muscle atrophy. *Cell Biochem Biophys* 2011;**60**:113–118.
16. Castillero E, Alamdari N, Lecker SH, Hasselgren PO. Suppression of atrogin-1 and MuRF1 prevents dexamethasone-induced atrophy of cultured myotubes. *Metabolism* 2013;**62**:1495–1502.
17. Clarke BA, Drujan D, Willis MS, Murphy LO, Corpina RA, Burova E, et al. The E3 ligase MuRF1 degrades myosin heavy chain protein in dexamethasone-treated skeletal muscle. *Cell Metab* 2007;**6**:376–385.
18. Gielen S, Sandri M, Kozarez I, Kratsch J, Teupser D, Thiery J, et al. Exercise training attenuates MuRF-1 expression in the skeletal muscle of patients with chronic heart failure independent of age: the randomized Leipzig Exercise Intervention in Chronic Heart Failure and Aging (LEICA) catabolism study. *Circulation* 2012;**125**:2716–2727.
19. Bowen TS, Adams V, Werner S, Fischer T, Vinke P, Brogger MN, et al. Small-molecule inhibition of MuRF1 attenuates skeletal muscle atrophy and dysfunction in cardiac cachexia. *J Cachexia Sarcopenia Muscle* 2017;**8**:939–953.
20. Bowen TS, Mangner N, Werner S, Glaser S, Kullnick Y, Schrepper A, et al. Diaphragm muscle weakness in mice is early-onset post-myocardial infarction and associated with elevated protein oxidation. *J Appl Physiol* 2015;**118**:11–19.
21. Mangner N, Weikert B, Bowen TS, Sandri M, Höllriegel R, Erbs S, et al. Skeletal muscle alterations in chronic heart failure: differential effects on quadriceps and diaphragm. *J Cachexia Sarcopenia Muscle* 2015;**6**:381–390.
22. Mangner N, Bowen TS, Werner S, Fischer T, Kullnick Y, Oberbach A, et al. Exercise training prevents diaphragm contractile dysfunction in heart failure. *Med Sci Sports Exerc* 2016;**48**:2118–2124.
23. Cox J, Mann M. MaxQuant enables high peptide identification rates, individualized p.p.b.-range mass accuracies and proteome-wide protein quantification. *Nat Biotechnol* 2008;**26**:1367–1372.
24. Elias JE, Gygi SP. Target-decoy search strategy for increased confidence in large-scale protein identifications by mass spectrometry. *Nat Methods* 2007;**4**:207–214.
25. Boersema PJ, Raijmakers R, Lemeer S, Mohammed S, Heck AJR. Multiplex peptide stable isotope dimethyl labeling for quantitative proteomics. *Nat Protoc* 2009;**4**: 484–494.
26. Hirner S, Krohne C, Schuster A, Hoffmann S, Witt S, Erber R, et al. MuRF1-dependent regulation of systemic carbohydrate metabolism as revealed from transgenic mouse studies. *J Mol Biol* 2008;**379**: 666–677.
27. Mukherjee A, Srere PA, Frenkel EP. Studies of the mechanism by which hepatic citrate synthase activity increases in vitamin B12 deprivation. *J Biol Chem* 1976;**251**: 2155–2160.
28. Vanderlinde RE. Measurement of total lactate dehydrogenase activity. *Ann Clin Lab Sci* 1985;**15**:13–31.
29. Dzeja PP, Pucar D, Redfield MM, Burnett JC, Terzic A. Reduced activity of enzymes coupling ATP-generating with ATP-consuming processes in the failing myocardium. *Mol Cell Biochem* 1999;**201**: 33–40.
30. Takashi O, Takashi H. Occurrence of two 3-hydroxyacyl-CoA dehydrogenases in rat liver. *Biochim Biohphys Acta* 1979;**574**: 258–267.
31. Schwarzer M, Osterholt M, Lunkenbein A, Schrepper A, Amorim P, Doenst T. Mitochondrial reactive oxygen species production and respiratory complex activity in

rats with pressure overload-induced heart failure. *J Physiol* 2014;**592**:3767–3782.
32. Mrosek M, Labeit D, Witt S, Heerklotz H, von Castelmur E, Labeit S, et al. Molecular determinants for the recruitment of the ubiquitin-ligase MuRF-1 onto M-line titin. *FASEB J* 2007;**21**:1383–1392.
33. Schauer A, Adams V, Poitz DM, Barthel P, Joachim D, Friedrich J, et al. Loss of Sox9 in cardiomyocytes delays the onset of cardiac hypertrophy and fibrosis. *Int J Cardiol* 2019;**282**:68–75.
34. Dobin A, Davis CA, Schlesinger F, Drenkow J, Zaleski C, Jha S, et al. STAR: ultrafast universal RNA-seq aligner. *Bioinformatics* 2013;**29**:15–21.
35. Anders S, Pyl PT, Huber W. HTSeq—a Python framework to work with high-throughput sequencing data. *Bioinformatics* 2015;**31**:166–169.
36. Love MI, Huber W, Anders S. Moderated estimation of fold change and dispersion for RNA-seq data with DESeq2. *Genome Biol* 2014;**15**:550–571.
37. Ribeiro JP, Chiappa GR, Neder JA, Frankenstein L. Respiratory muscle function and exercise intolerance in heart failure. *Curr Heart Fail Rep* 2009;**6**:95–101.
38. Hughes PD, Polkey MI, Lou Harries M, Coats AJS, Moxham J, Green M. Diaphragm strength in chronic heart failure. *Am J Respir Crit Care Med* 1999;**160**:529–534.
39. Bowen TS, Rolim NPL, Fischer T, Baekkerud FH, Medeiros A, Werner S, et al. Heart failure with preserved ejection fraction induces molecular, mitochondrial, histological, and functional alterations in rat respiratory and limb skeletal muscle. *Eur J Heart Fail* 2015;**17**:263–272.
40. Lecker SH. Ubiquitin–protein ligases in muscle wasting: multiple parallel pathways? *Curr Opin Clin Nutr Metab Care* 2004;**6**:271–275.
41. Bowen TS, Schuler G, Adams V. Skeletal muscle wasting in cachexia and sarcopenia: molecular pathophysiology and impact of exercise training. *J Cachexia Sarcopenia Muscle* 2015;**6**:197–207.
42. Bonaldo P, Sandri M. Cellular and molecular mechanisms of muscle atrophy. *Dis Model Mech* 2013;**6**:25–39.
43. Levine S, Biswas C, Dierov J, Barsotti R, Shrager JB, Nguyen T, et al. Increased proteolysis, myosin depletion, and atrophic AKT–FOXO signaling in human diaphragm disuse. *Am J Respir Crit Care Med* 2011;**183**:483–490.
44. Hooijman PE, Beishuizen A, Witt CC, de Waard MC, Girbes ARJ, Spoelstra-de Man AME, et al. Diaphragm muscle fiber weakness and ubiquitin–proteasome activation in critically ill patients. *Am J Respir Crit Care Med* 2015;**191**:1126–1138.
45. Le Dinh M, Carreira S, Obert J, Gayan-Ramirez G, Riou B, Beuvin M, et al. Prolonged mechanical ventilation worsens sepsis-induced diaphragmatic dysfunction in the rat. *PLoS ONE* 2018;**13**:e0200429.
46. van Hees HWH, Schellekens WJ, Andrade Acuna GL, Linkels M, Hafmans T, Ottenheijm CAC, et al. Titin and diaphragm dysfunction in mechanically ventilated rats. *Intensive Care Med* 2012;**38**:702–709.
47. van den Berg M, Hooijman PE, Beishuizen A, de Waard MC, Paul MA, Hartemink KJ, et al. Diaphragm atrophy and weakness in the absence of mitochondrial dysfunction in the critically ill. *Am J Respir CritCare Med* 2017;**196**:1544–1558.
48. Ahn B, Empinado HM, Al-Rajhi M, Judge AR, Ferreira LF. Diaphragm atrophy and contractile dysfunction in a murine model of pulmonary hypertension. *PLoS ONE* 2013;**8**:e62702.
49. Demoule A, Jung B, Prodanovic H, Molinari N, Chanques G, Coirault C, et al. Diaphragm dysfunction on admission to the intensive care unit. Prevalence, risk factors, and prognostic impact—a prospective study. *Am J Respir CritCare Med* 2013;**188**:213–219.
50. Noh KK, Chung KW, Choi YJ, Park MH, Jang EJ, Park CH, et al. β-Hydroxy β-methylbutyrate improves dexamethasone-induced muscle atrophy by modulating the muscle degradation pathway in SD rat. *PLoS ONE* 2014;**9**:e102947.
51. Yakabe M, Ogawa S, Ota H, Iijima K, Eto M, Ouchi Y, et al. Inhibition of interleukin-6 decreases atrogene expression and ameliorates tail suspension-induced skeletal muscle atrophy. *PLoS ONE* 2018;**13**:e0191318.
52. Belova SP, Shenkman BS, Kostrominova TY, Nemirovskaya TL. Paradoxical effect of IKKβ inhibition on the expression of E3 ubiquitin ligases and unloading-induced skeletal muscle atrophy. *Physiol Rep* 2017;**5**:e13291.
53. Caron AZ, Haroun S, Leblanc E, Trensz F, Guindi C, Amrani A, et al. The proteasome inhibitor MG132 reduces immobilization-induced skeletal muscle atrophy in mice. *BMC Musculoskelet Disord* 2011;**12**:185.
54. Zhang L, Tang H, Kou Y, Li R, Zheng Y, Wang Q, et al. MG132-mediated inhibition of the ubiquitin–proteasome pathway ameliorates cancer cachexia. *J Cancer Res Clin Oncol* 2013;**139**:1105–1115.
55. Jamart C, Raymackers JM, Li An G, Deldicque L, Francaux M. Prevention of muscle disuse atrophy by MG132 proteasome inhibitor. *Muscle Nerve* 2011;**43**:708–716.
56. Supinski GS, Vanags J, Callahan LA. Effect of proteasome inhibitors on endotoxin-induced diaphragm dysfunction. *Am J Physiol Lung Cell Mol Physiol* 2009;L994–L1001.
57. Smuder AJ, Nelson WB, Hudson MB, Kavazis AN, Powers SK. Inhibition of the ubiquitin–proteasome pathway does not protect against ventilatory-induced accelerated proteolysis or atrophy in the diaphragm. *Anesthesiology* 2014;**121**:115–126.
58. Willis MS, Ike C, Li L, Wang DZ, Glass DJ, Patterson C. Muscle ring finger 1, but not muscle ring finger 2, regulates cardiac hypertrophy in vivo. *Circ Res* 2007;**100**:456–459.
59. Houtkooper RH, Mouchiroud L, Ryu D, Moullan N, Katsyuba E, Knott G, et al. Mitonuclear protein imbalance as a conserved longevity mechanism. *Nature* 2013;**497**:451–457.
60. Romanello V, Sandri M. Mitochondrial biogenesis and fragmentation as regulators of protein degradation in striated muscles. *J Mol Cell Cardiol* 2013;**55**:64–72.
61. Liu J, Peng Y, Cui Z, Wu Z, Qian A, Shang P, et al. Depressed mitochondrial biogenesis and dynamic remodelingin mouse tibialis anterior and gastrocnemius induced by 4-week hindlimb unloading. *IUBMB Life* 2012;**64**:901–910.
62. Bowen TS, Eisenkolb S, Drobner J, Fischer T, Werner S, Linke A, et al. High-intensity interval training prevents oxidant-mediated diaphragm muscle weakness in hypertensive mice. *FASEB J* 2016;**31**:60–71.
63. Laitano O, Ahn B, Patel N, Coblentz PD, Smuder AJ, Yoo JK, et al. Pharmacological targeting of mitochondrial reactive oxygen species counteracts diaphragm weakness in chronic heart failure. *J Appl Physiol* 2016;**120**:733–742.
64. Mcparland C, Krishnan B, Wang Y, Gallagher CG. Inspiratory muscle weakness and dyspnea in chronic heart failure. *Am Rev Respir Dis* 1992;**146**:467–472.
65. Seiler M, Bowen TS, Rolim N, Dieterlen MT, Werner S, Hoshi T, et al. Skeletal muscle alterations are exacerbated in heart failure with reduced compared with preserved ejection fraction: mediated by circulating cytokines? *Circ Heart Fail* 2016;e003027.
66. Carvalho RF, Castan EP, Coelho CA, Lopes FS, Almeida FLA, Michelin A, et al. Heart failure increases atrogin-1 and MuRF1 gene expression in skeletal muscle with fiber type-specific atrophy. *J Mol Histol* 2010;**41**:81–87.
67. Witt SH, Granzier H, Witt CC, Labeit S. Murf-1 and Murf-2 target a specific subset of myofibrillar proteins redundantly: towards understanding Murf-dependent ubiquitination. *J Mol Biol* 2005;**350**:713–722.
68. Polge C, Cabantous S, Deval C, Claustre A, Hauvette A, Bouchenot C, et al. A muscle-specific MuRF1–E2 network requires stabilization of MuRF1–E2 complexes by telethonin, a newly identified substrate. *J Cachexia Sarcopenia Muscle* 2018;**9**:129–145.
69. von Haehling S, Morley JE, Coats Andrew JS, Anker SD. Ethical guidelines for publishing in the *Journal of Cachexia, Sarcopenia and Muscle*: update 2017. *J Cachexia Sarcopenia Muscle* 2017;**8**:1081–1083.